Faraday Discussions

Cite this: *Faraday Discuss.*, 2017, **196**, 285

PAPER

Deciphering the binding behaviours of BSA using ionic AIE-active fluorescent probes†

Jiaqi Tong,[a] Ting Hu,[a] Anjun Qin,[b] Jing Zhi Sun*[a] and Ben Zhong Tang*[abc]

Received 29th June 2016, Accepted 25th July 2016
DOI: 10.1039/c6fd00165c

The binding behaviours of a transport protein, bovine serum albumin (BSA), in its native, unfolding and refolding states have been probed by monitoring the emission changes of two exogenous AIE-active fluorescent probes, **M2** and **M3**, which are designed to be anionic and cationic, respectively. Due to their AIE properties, both **M2** and **M3** display emission enhancement when bound to the hydrophobic cavity of BSA. The binding site of **M2** and **M3** is found to be subdomain IIA. Then, the BSA + **M2** and BSA + **M3** systems are utilized to fluorescently signal the conformation changes of BSA caused by various external stimuli, including thermally or chemically induced denaturation. The data confirmed the multi-step unfolding process and the existence of a molten-globule intermediate state. The unfolding process consists of the rearrangement of subdomain IIA, the exposure of a negatively charged binding site in domain I that prefers interacting with cationic species, and the transformation of the molten-globule intermediate into the final random coil. The anionic and cationic modifications of the probes enable us to observe that electrostatic interactions play a role in the folding and unfolding of BSA.

Introduction

Serum albumin (SA), as the most abundant circulatory protein in plasma, is involved in various metabolic processes, such as determining plasma oncotic pressure, modulating fluid distribution, antagonizing the activity of toxins and

[a]*MoE Key Laboratory of Macromolecular Synthesis and Functionalization, Department of Polymer Science and Engineering, Zhejiang University, Hangzhou 310027, China. E-mail: sunjz@zju.edu.cn*

[b]*Guangdong Innovative Research Team, State Key Laboratory of Luminescent Materials and Devices, South China University of Technology, Guangzhou 510640, China*

[c]*Division of Biomedical Engineering, Department of Chemistry, Hong Kong Branch of Chinese National Engineering Research Center for Tissue Restoration and Reconstruction, Institute for Advanced Study, Division of Life Science, Institute of Molecular Functional Materials and State Key Laboratory of Molecular Neuroscience, The Hong Kong University of Science & Technology (HKUST), Clear Water Bay, Kowloon, Hong Kong, China. E-mail: tangbenz@ust.hk*

† Electronic supplementary information (ESI) available: Conformational structure of BSA in its native state, and fluorescence spectra for the mixtures of BSA and **M2**/**M3** under different conditions. See DOI: 10.1039/c6fd00165c

controlling the anti-oxidant properties of plasma.[1] More remarkably, SA exhibits an outstanding binding capacity for loading and transporting many endogenous and exogenous compounds.[2] In addition to being the major transport protein for fatty acids,[3] SA also binds diverse metabolites, organic compounds and drugs, which gives it a central role in pharmaceutics or drug pharmacokinetics.[4] SA aids the dissolution of hydrophobic compounds, the distribution of ligands throughout the whole body, and the resistance of these ligands to being metabolized.[5] Bovine serum albumin (BSA), a kind of homologous protein of serum albumin, consists of 583 amino acid residues and forms a single polypeptide chain. BSA adopts a heart-shaped structure, consisting of about 67% α-helix and seventeen disulphide bridges, and it is divided into three homologous domains (I, II and III), which are further partitioned into two subdomains, A and B (Fig. S1†).[6] As a typical SA, BSA is an area of intense current research, since it is a reference for the study of SA or human serum albumin (HSA) and can be used as a model for understanding the basic principles of protein issues. Reasonably, elucidating the properties of BSA can help us in better understanding the properties of HSA and designing new albumins with improved functionality, which can even be used as a substitute for HSA.[7] Moreover, not only are the various binding aspects of serum albumins considered, but also the conformational dynamics of the protein towards diverse stimuli are followed, since this is conducive to controlling the efficient delivery of drugs and, more importantly, to deeply understanding the functional principles of proteins at the molecular level.[8]

A number of works dealing with the binding of sundry ligands to BSA/HSA have been reported by using techniques such as circular dichroism spectroscopy, nuclear magnetic resonance, fluorescent spectroscopy and so forth.[9,10] Among them, fluorescent spectroscopy is widely applied, based on the intrinsic fluorescence from BSA or the extrinsic fluorescence from a variety of binding fluorogens.[10] The fluorogens displaying changes in emission features (intensity, wavelength and/or lifetime) can be used to signal the binding process of themselves to BSA and act as non-covalent labels of BSA. Through the detectable feature changes, information about the binding aspects of BSA has been successfully collected in a certain amount of detail. However, the studies based on fluorescent probes are still limited because of the lack of high performance fluorogens or dyes. For example, there exists a problem that some dyes emit less efficiently when binding to the pockets or cavities of proteins than dispersed in aqueous media.[11] Others change their emission colors when they bind to the target proteins. Normally, this kind of fluorescent probe shows a blue-shifted emission band in the hydrophobic pocket of the binding protein, in comparison with the more hydrophilic environment before binding. As a result, the environment-sensitive fluorescent probes offer a unique colorimetric method to signal the binding process.

In 2006, a new kind of fluorescent probe with aggregation-induced emission (AIE) properties was reported to be used in the fluorescent detection of BSA.[12] In a typical AIE process, the weakly emissive fluorogens are induced to emit strongly by the formation of aggregates. The mechanistic studies revealed that the restriction of intramolecular motion (RIM) processes accounts for the AIE phenomenon. So far, the RIM processes can be mainly classified into two specific situations, which are the restricted intramolecular rotations (RIR) and restricted intramolecular vibrations (RIV) for propeller- and shell-like luminogen systems,

respectively.[13] As shown in Chart 1, the first reported AIE-active luminogen or AIEgen used in BSA detection was a tetraphenylethene (TPE) derivative (**M1**).[12] Due to the two quaternary ammonium cations, **M1** is soluble in aqueous buffer solutions and shows faint fluorescence. However, the TPE core is intrinsically hydrophobic. Once the probe molecules are engulfed by the hydrophobic pockets of BSA or HSA, the RIM effect of the propeller-shaped TPE luminogen takes over and the molecules become highly fluorescent. According to the AIE mechanism, BSA or HSA is detected by reading the variation of the fluorescence intensity.

The molecular design was renewed by H. Tong *et al.* through replacing the two quaternary ammonium cations with two sulphonate anions (**M2**, Chart 1),[14] because the sensitivity of **M1** in the detection of proteins was undesirable. BSA could be detected at a concentration as low as 500 ng mL^{-1} by using **M2** as a fluorescent probe. The calibration curve exhibited a fairly wide linear range (0–100 μg mL^{-1}). A significant observation was that the fluorescence of **M2** could not be turned on by denatured BSA. Thus the fluorescence enhancement in the presence of BSA was rationally associated with the binding of **M2** to the hydrophobic pockets within BSA, which disappeared in the denatured state. Based on this detection mechanism, it was envisioned that even lower BSA levels could be detectable at higher **M2** concentration without suffering from the self-quenching problem of traditional organic dyes. By introducing TPE moieties into the side chains of a water soluble polymer, the detection sensitivity to BSA was further boosted up to an ultra-high level of 0–0.6 ppm.[15]

Besides the unique detection mechanism and high sensitivity, BSA detection with AIE-active probe **M2** showed other advantages. For example, the

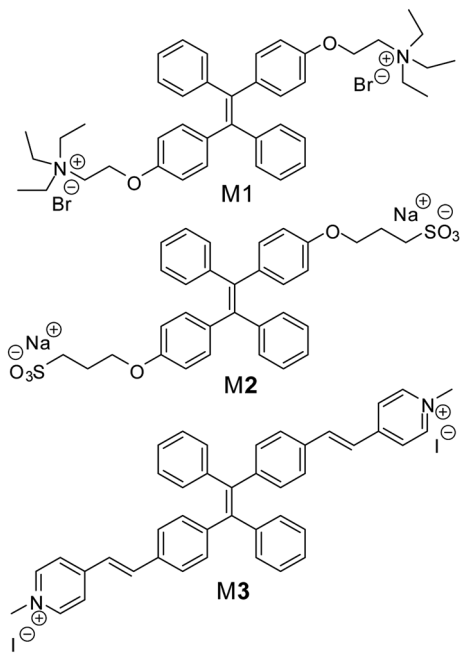

Chart 1 Chemical structure of the AIE-active fluorescent probes.

detection is not interfered with by the presence of different bioelectrolytes in artificial urine. Thus the methodology is put to use in the investigation of different processes of proteins, such as the visualization of the hydrophobic pockets of proteins and the catalytic sites of enzymes, the monitoring of the conformational changes and amyloid fibrillation process, and the specific binding of cyclic arginine–glycine–aspartic acid (cRGD) towards integrin $\alpha_v\beta_3$.[16] A study on the conformational transitions of human serum albumin (HSA) was also tried.[17] The weakly emissive **M2** in buffer solution became strongly emissive upon the addition of native HSA, but the emission could not be triggered out by HSA in the presence of guanidine. Combining the RIR and Forster resonance energy transfer mechanism, the unfolding process of HSA was elucidated in unprecedented detail.[17] With increasing concentration of the denature agent guanidine hydrochloride (GndHCl), the native HSA underwent a multi-step transition process involving domain separation, a molten globule and finally the unfolded coil.

Despite this substantial progress, further understanding of the BSA–ligand binding process and the conformational transitions between the native and denatured states is still of great scientific significance. For example, both dicationic and dianionic AIE-active fluorogens (**M1** and **M2**) have been used in the previous works, and they clearly showed fluorescent responses to BSA binding. Given that BSA is a transportation protein possessing different pockets, do the cationic and anionic probes bind to the same hydrophobic pocket of BSA? If yes, can we conclude that the binding of fluorogens to BSA depends solely on the hydrophobic effect? If not, what is the role of the charged groups in the binding process? Furthermore, it is assumed that some proteins undergo a hysteresis loop of the folding → unfolding → refolding process. Can we acquire further understanding of the folding → unfolding → refolding behaviours of BSA?

In the hope of further understanding the above issues, two TPE-derivatives are used to study the detailed processes of interest in this work and their structures (**M2** and **M3**) are shown in Chart 1. **M2** is used in the present work for its excellent sensitivity of fluorescent response to BSA as reported in the literature.[14] The reason for the choice of **M3** is based on two considerations: (1) in previous work, it was noted that the cationic **M1** had lower sensitivity than the anionic **M2**.[14,15] The difference in sensitivity may be associated with the difference in the size of the charged species. For **M1**, the positive charge localizes inside the bulky triethylbutyl-ammonium group. According to Coulomb's law, the strength of electrostatic attraction follows the inverse square law, and the bulky size of triethylbutylammonium would weaken the Coulomb force thereby resulting in lower sensitivity. For **M3**, the pyridinium cation has a smaller size than the triethylbutyl-ammonium moiety and it is exposed directly to its surroundings. We thus expect that **M3** will display higher sensitivity than **M1**. (2) **M1** and **M2** emit identical fluorescence because they have the same luminogen, although they bear opposite static charges. **M3** is composed of a TPE core and two pyridinium moieties. The C=C double-bond linkage expands the effective conjugation hence allowing **M3** to emit red-shifted fluorescence. The difference in emission color benefits the examination of relevant processes using **M2** and **M3** concomitantly.

Experimental section

Chemicals

The synthetic routes to the anionic and cationic TPE derivatives (**M2** and **M3**) and their AIE behaviors have been reported elsewhere.[14,18] Unless otherwise noted, all reagents were purchased from commercial suppliers and used without further purification. The purchased BSA was further purified according to the literature[19] so as to make the protein free of fatty acids. Routine phosphate buffer (containing 10 mM Na_2HPO_4, 2 mM KH_2PO_4, 137 mM NaCl and 2.7 mM KCl) was prepared by dissolving the corresponding components in deionized water and adjusting the pH to a final value of 7.40. The phosphate buffers used to study influence of pH on the folding of BSA were prepared by mixing certain amounts of H_3PO_4, NaH_2PO_4 or Na_2HPO_4 in deionized water and adjusting the pH to specified values with NaOH or HCl. Stock solutions of **M2** and **M3** were prepared by dissolving appropriate amounts of the two probes in the aqueous phosphate buffer to a concentration of 20 μM. The stock solution of BSA (20 μM) in phosphate buffer was prepared based on its molecular weight of 66.4 kDa and the concentration was further checked by measuring the absorbance at 280 nm with an extinction coefficient of 44 720 M^{-1} cm^{-1}.[14]

Measurements

For fluorescence (FL) titration, aliquots of a BSA solution were added to 1 mL of an **M2** or **M3** solution, which was then diluted with phosphate buffer to a final volume of 10 mL. For energy transfer experiments, the BSA concentration was fixed at 1 μM while a set of the dye solutions with increasing amounts was added and finally diluted to the concentration of 0–10 μM. For thermal denaturation, the concentration of the probes and BSA were kept at 1 μM, and the samples were incubated at the designated constant temperature for 10 min before taking the measurements through an accessional water bath. For the unfolding experiments caused by urea or guanidine hydrochloride, a series of diluted solutions of the denaturants with varied concentrations were sequentially mixed with certain amounts of BSA and a probe, both of which have a final constant concentration of 1 μM. For pH-induced unfolding, BSA and the probes were first mixed with phosphates (H_3PO_4, NaH_2PO_4 or Na_2HPO_4) in deionized water and then the pH of the solutions was adjusted to specified values with NaOH or HCl. Except for the thermal denaturation experiments, all the samples were incubated for 30 min to achieve equilibrium prior to the measurements and all the measurements were carried out at ambient temperature (~25 °C). FL spectra were recorded using a Shimadzu RF-5301PC spectrofluorophotometer. UV-vis absorption spectra were recorded using a Varian VARY 100 Bio UV-vis spectrophotometer.

Results and discussion

Confirmation of the binding of M2 and M3 to BSA

The binding of **M2** to BSA has been reported in the previous work.[14] To keep the experimental conditions consistent in the present work, we set the pH value of the phosphate buffer solution at 7.4 as the common condition, which was composed of 10 mM Na_2HPO_4, 2 mM KH_2PO_4, 137 mM NaCl, 2.7 mM KCl and deionized

water. The emission behaviour of **M2** (1.0 μM) was examined in aqueous phosphate buffer solution (pH 7.4) with different concentrations of BSA (referred to as the BSA + **M2** system below). As shown in Fig. 1A and B, **M2** emits weakly in the buffer solution and the emission peak appears at 459 nm. After the addition of BSA into the buffer solution containing 1.0 μM of **M2**, the emission intensity is immediately boosted and the emission peak red-shifts to around 476 nm. The changes of FL intensity can be intuitively revealed by the photographs of the inset of Fig. 1B, which shows the obviously enhanced greenish-blue emission from the buffer solution containing BSA. Quantitatively, the FL intensity recorded for the system containing 0.1 μM of BSA increases to about 10 times that recorded in the absence of BSA. When the BSA concentration increases to about 0.6 μM, the emission achieves saturation intensity, and about a 12-fold enhancement was recorded. These characteristics are in good agreement with the results reported in previous works,[14] indicating that the changes in FL features are convincing messages to signal the binding between BSA and **M2**.

Under the same experimental conditions, the variation of the emission features of **M3** (1 μM) upon addition of different concentrations of BSA (referred to as the BSA + **M3** system below) are demonstrated in Fig. 2A and B. The general trends of the emission features are similar to those observed in the BSA + **M2** system. **M3** is faintly emissive in buffer solution in the absence of BSA. On increasing the concentration of BSA, the FL intensity grows stronger and stronger. According to the RIR mechanism and the understanding derived from our previous works, **M3** can also be used as a fluorescent reporter of the BSA–probe interaction. However, the details of the emission features of the BSA + **M3** system demonstrate some differences from the BSA + **M2** system.

Firstly, the emission peak of **M3** in phosphate buffer solution appears at around 573 nm, indicating an orange emission. The wavelength gap between **M2**

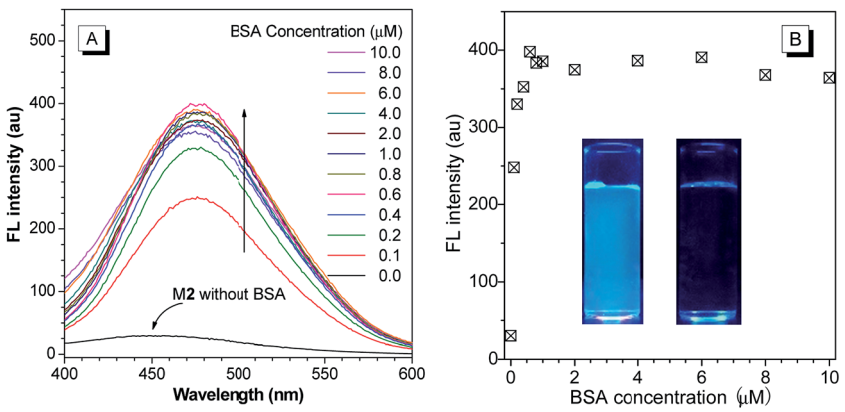

Fig. 1 (A) Fluorescence (FL) spectra of **M2** in aqueous phosphate buffer solution (pH 7.4) with different concentrations of BSA. (B) Variation of FL peak intensity with BSA concentration, in which the data are extracted from the spectra shown in (A) at an emission wavelength of 459 nm for the sample without BSA and 476 nm for the other samples. Excitation wavelength (λ_{ex}): 330 nm; **M2** concentration ([**M2**]): 1 μM. Inset of (B): photographs showing the emission of **M2** in buffer solution (pH 7.4) with and without BSA taken under illumination with 365 nm UV-light.

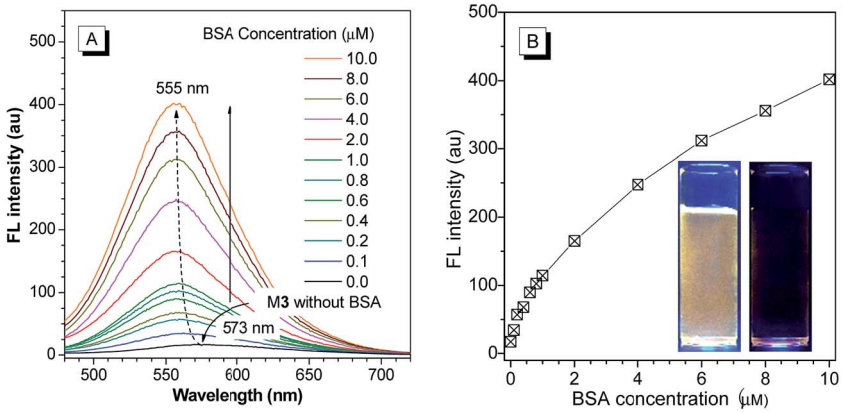

Fig. 2 (A) FL spectra of **M3** in aqueous phosphate buffer solution (pH 7.4) with different concentrations of BSA. (B) Variation of FL peak intensity with BSA concentration, in which the data are extracted from the spectra shown in (A). Excitation wavelength (λ_{ex}): 395 nm; [**M3**] = 1 μM. Inset of (B): photographs showing the emission of **M3** in buffer solution (pH 7.4) with and without BSA taken under illumination with 365 nm UV-light.

and **M3** is nearly 100 nm, which can be easily recognized by their emission colors and thus it is helpful to use them simultaneously in the comparative study of BSA binding events. Meanwhile, the emission intensity of the BSA + **M3** system is comparative to that of BSA + **M2** when the concentration of BSA is 4.0 M, indicating that **M3** is better than **M1**. Secondly, when adding BSA to the **M3**-containing solution, the emission peak appears at around 555 nm, indicating a blue-shift of 18 nm (573 to 555 nm). This is distinct from those observed for the BSA + **M1** and BSA + **M2** systems. The fluorophore of both **M1** and **M2** is a TPE moiety with two electron donating alkyloxyl groups, but the fluorophore of **M3** is not a TPE moiety but an extended conjugation system with two pyridinium moieties conjugating with the TPE core. Because of the enlarged molecular size of **M3**, we tentatively infer that the conformation of **M3** should be more twisted when it binds to BSA in order to be accommodated by the hydrophobic pocket. Thirdly, comparing the plots in Fig. 1B and 2B shows that the emission intensity of the BSA + **M3** system enhances gradually with the increase of BSA concentration, but for the BSA + **M2** system the emission intensity grows steeply with the addition of BSA. The difference implies that the interaction mode between BSA and **M2** may be distinct from that of BSA and **M3**.

Estimation of the binding constants of M2 and M3 to BSA

The emission enhancement of **M2** and **M3** in the presence of BSA has disclosed some information about the binding of the probes to BSA, but the detailed binding mechanisms such as the binding constant and binding sites need to be further and carefully explored.

To elucidate these issues, the principle of fluorescence resonance energy transfer between BSA and **M2** or **M3** is adopted. BSA has three fluorophores, which are tryptophan (Trp), tyrosine (Tyr) and phenylalanine (Phe). The intrinsic fluorescence of BSA is mainly attributed to the Trp residue, because of the

particularly weak fluorescence of Phe and the nearly totally quenched fluorescence of the Tyr residue. BSA contains two Trp residues, *i.e.* Trp-134 and Trp-212, locating in the IB and IIA subdomains, respectively (Fig. S1†).[20] According to the theory of Förster's resonance energy transfer (FRET), efficient energy transfer occurs if there exists a certain degree of spectral overlap between the emission band of the donor and the absorption band of the acceptor and meanwhile the distance between the donor and acceptor is within 2–8 nm. Based on the FRET principle, the emission intensity of the donor and acceptor would gradually decrease and increase, respectively, as the concentration of the acceptor increases.[21]

The changes in the intrinsic fluorescence of BSA with adding increasing amounts of **M2** or **M3** have been measured and the recorded data are depicted in Fig. 3 and S2.† The FL spectrum of the native BSA displays a single band with a peak at 345 nm. After a certain concentration of **M2** or **M3** was mixed with BSA, the FL from BSA became weaker. The quenching of BSA's fluorescence by adding **M2** or **M3** is associated with the energy transfer from the protein's fluorophores to **M2** or **M3**. In order to quantitatively evaluate the protein–probe interactions, the quenching data of BSA fluorescence were examined using the Stern–Volmer equation:[22]

$$\frac{F_0}{F} = 1 + K_{sv}[Q] \quad (1)$$

where F_0 and F are the emission intensities of the fluorophore (Tyr in BSA) in the absence and presence of the quencher (**M2** or **M3**), [Q] and K_{sv} stand for the quencher concentration and the Stern–Volmer quenching constant, respectively. Based on eqn (1), the binding constant and binding affinity of the probes for BSA can be further estimated with a modified version of the Stern–Volmer equation which is given by:

$$\log\frac{F_0 - F}{F} = \log K + n\log[Q] \quad (2)$$

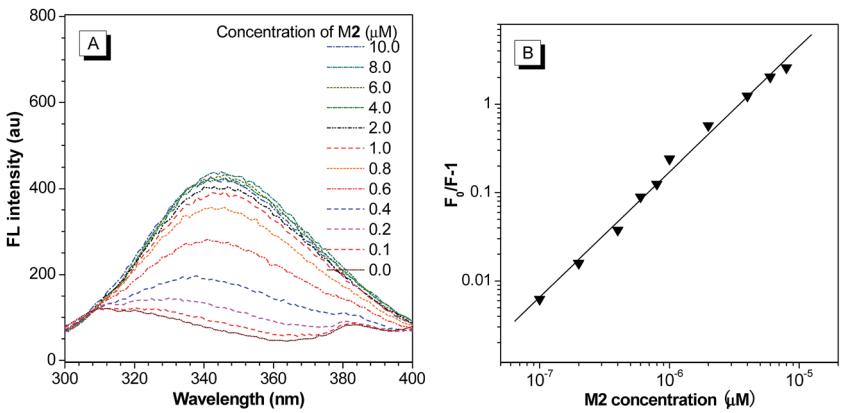

Fig. 3 (A) Fluorescence (FL) spectra of BSA in the presence of different [**M2**]. (B) Plot of lg $[(F_0 - F)/F]$ *vs.* lg[**M2**]; F_0 and F: the peak FL intensity of BSA without **M2** and with different [**M2**] values. BSA concentration: 1 μM; λ_{ex}: 280 nm.

where K and n are the binding constant and the number of binding sites, respectively. According to eqn (2), the plot of $\log[(F_0 - F)/F]$ *versus* $\log[Q]$ is calculated and shown in Fig. 3B. For the complex BSA + **M2**, the calculated values of the binding constant (K) and the number of binding sites (n) are 5.50×10^7 L mol^{-1} and 1.42, respectively. For the complex BSA + **M3**, the K and n values are 1.38×10^6 L mol^{-1} and 1.21, respectively (Fig. S2†). The numerical values of n indicate that only one binding site in native BSA is involved with the binding of **M2** or **M3**.

Estimation of the binding sites of M2 and M3 to BSA

Based on the above data, the exact binding sites of the two probes in BSA can be further checked. The two fluorophores, Trp-134 and Trp-212, are located in subdomains IB and IIA, respectively. Accordingly, the probes are likely to bind to subdomains IB and IIA. In other words, domains bound by **M2** or **M3** are approximate to where the fluorophores localize, since no fluorescence quenching is expected to occur if the probes bind to sites that are far away from Trp-134 or Trp-212.

Besides the FRET strategy, the replacing effect of various known site-selective binding ligands on the binding of **M2** or **M3** was examined to help understand the binding process. If the ligand binds to the same region as the probes in BSA, the ligand has a competitive effect or an inhibitory effect on the interaction of **M2** or **M3** and BSA. Namely, adding the ligand to the BSA–**M2** or BSA–**M3** complex can cause exchange between the ligand and the probe molecules thereby gradual decreasing the fluorescence intensity. Based on this idea, the effect of ligand addition on the interaction of **M2** and BSA was studied. Previous works reported that there is more than one binding site for fatty acids in BSA with different degrees of affinity to the ligands.[23] It has been confirmed that BSA has three high affinity sites or three primary binding sites to myristic acid (a fatty acid), which consist of one site in subdomain IIIA, one in subdomain IIIB and one at the interface between subdomain IA and IIA. The change in fluorescence intensity of **M2** in BSA solutions which had been incubated with increasing amounts of myristic acid was monitored (Fig. S3†). The obtained results demonstrated that almost no change in the emission intensity of **M2** had occurred. This observation indicated that there was no exchange between myristic acid and the **M2** molecules, therefore it can be inferred that **M2** binds to a site (or some sites) different from the binding sites specifically for myristic acid. Therefore, it can be concluded that the binding event of BSA to **M2** has not occurred at the high affinity sites of BSA to myristic acid (subdomain IIIA, subdomain IIIB and the interface between subdomains IA and IIA). Similar experiments have been carried out on the BSA + **M3** system. Due to the electrostatic interaction between **M3** and myristic acid, the mixture of **M3** and myristic acid showed emission enhancement when the concentration of myristic acid was increased to a certain threshold ($\sim 6 \times 10^{-6}$ mol L^{-1}) (Fig. S4A and S4C†). In the presence of BSA, the **M3** probe is mostly encapsulated in a certain hydrophobic domain of BSA, and this domain must have a weak binding capacity for myristic acid. As a result, **M3** is seldom replaced by myristic acid molecules and the electrostatic interaction with myristic acid molecules becomes much weaker. Therefore, the emission behaviour of **M3** + myristic acid in the presence of BSA (Fig. S4B†) is different from that observed in the case of the absence of BSA, but similar to that displayed in Fig. S3.† According

to these results, we can conclude that the binding of **M3** to BSA does not occur at the same sites as myristic acid, *i.e.* the sites of subdomain IIIA, subdomain IIIB, and the interface between subdomain IA and IIA.

Then the two principle drug binding sites, subdomains IIA and IIIA were checked, which were reported in the pioneering work of Sudlow and thereby named as Sudlow I and II.[24] Since the above-mentioned data has shown that Sudlow II is hardly a binding site of **M2** and **M3**, the displacing effect of site-selective binding ligands for Sudlow I, such as warfarin, on the binding of **M2** and **M3** was investigated. After adding warfarin to the solution of BSA–**M2** complex, a gradual decrease in the fluorescence intensity corresponding to **M2** at 475 nm is observed. This process is accompanied by an emission enhancement of warfarin (Fig. 4A). A similar effective displacement in the case of warfarin and the BSA–**M3** complex has also been found (Fig. 4B). According to the RIM mechanism of AIE-activity, the decrease in FL intensity of **M2** and **M3** can be ascribed to the release of **M2** and **M3** from the binding site of BSA, which emancipates the movement restriction of the fluorogens in the binding state. This release is obviously caused by the displacement of **M2** and **M3** with warfarin. Thus, it is concluded that the two probes, both **M2** and **M3**, are bound to the Sudlow I or subdomain IIA of BSA, which is a principle drug binding site.

Thermal denaturation of BSA signaled using M2 and M3 as extrinsic fluorescent probes

According to the derived results, the negatively charged probe **M2** and positively charged probe **M3** show identical binding performance to BSA in the native state. It seems that the binding event only correlates with the hydrophobic effect of the binding site, regardless of the electrostatic interaction. In fact, electrostatic interaction plays crucial roles in many protein-related biological processes. It has been well-accepted that information about the binding of proteins to ligands can be inferred from their denaturation processes. As one of the characteristic

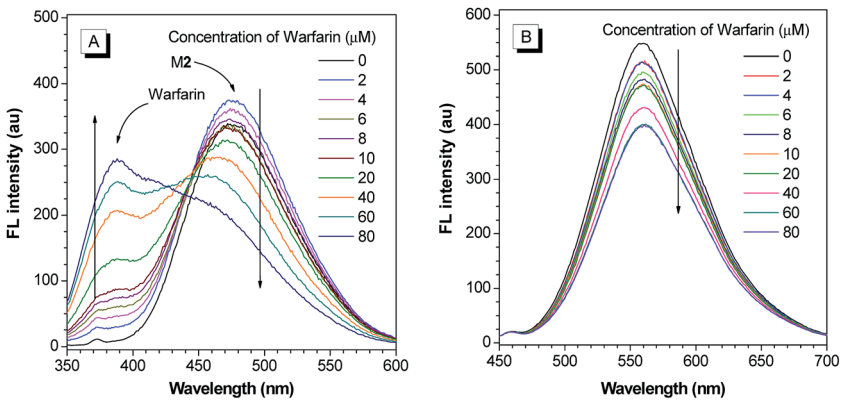

Fig. 4 (A) FL spectra of the BSA + **M2** system in the presence of warfarin, λ_{ex}: 330 nm, concentration of BSA: 1 μM. (B) FL spectra of the BSA + **M3** system in the presence of warfarin, λ_{ex}: 395 nm. Concentration of warfarin: 0–80 μM; concentration of BSA: 1 μM; concentration of **M2** or **M3**: 5 μM.

properties of proteins, thermal denaturation may cause the native protein structure to be disrupted and lose its functional conformation.[25] A comprehensive study of the thermal stability of proteins (including BSA) will be conducive to understanding the biological regulation and function mechanisms of the proteins responding to stimuli from the internal and external environment. By dint of the fluorescent characteristics of the two probes when bound to BSA discussed above, we detected the structure changes and ligand-binding properties of BSA in the unfolding and refolding processes impacted by rising and falling temperature.

The peak emission intensity and emission spectra of BSA + **M2** at different temperatures ranging from 25 °C to 70 °C are displayed in Fig. 5A and S5.† A monotonous reduction of the emission intensity was observed with the elevation of temperature. When it comes to the system of BSA + **M3** (Fig. 5B and S6†), an initial reduction of fluorescence intensity, which is similar to the case of BSA + **M2**, is followed by a palpable enhancement of the intensity as the temperature reached over 45 °C. Then the intensity goes through a subsequent decrease when the temperature increases to 60 °C or above. Given the fact that the fluorescence intensity of the two AIE-active probes themselves decreases as the temperature rises, the attenuation of the emission intensity of the two complexes cannot be directly and fully attributed to a structural change in the binding site. However, the dissimilar enhancement in the case of BSA–**M3** indicated that there does exist an intermediate state at around 50 °C, which has something to do only with probe **M3**.

The refolding processes of BSA in the two systems when lowering the temperature from 70 °C to room temperature were then recorded based on the conversions of emission properties (Fig. 5B). As the BSA + **M2** system was cooled from 70 °C to ambient temperature, the fluorescence intensity ascended, though it did not return to the original intensity before the heating–cooling cycle. This

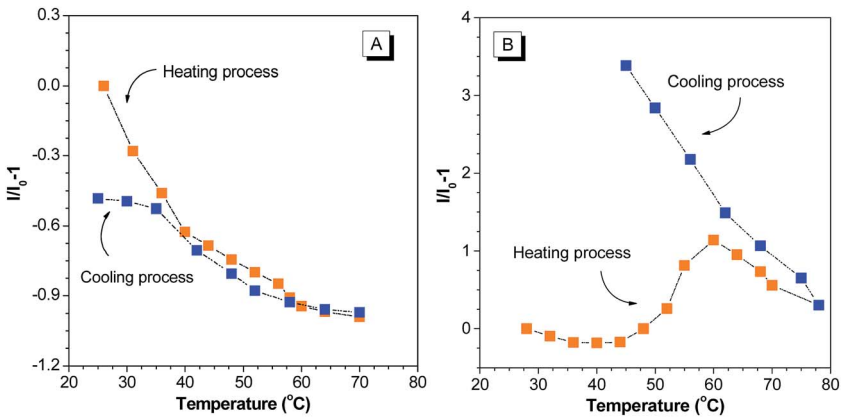

Fig. 5 Plots of the relative fluorescent intensities (I/I_0) of (A) BSA + **M2** and (B) the BSA + **M3** system in PBS buffer (pH = 7.4) as a function of temperature in the heating (from 25 °C to 75 °C, orange) and subsequent cooling processes (from 75 °C to 25 °C, blue). I_0 and I: the peak FL intensity of the system at 25 °C and at different temperatures. λ_{ex}: 330 nm for **M2** and 395 nm for **M3**; concentration of **M2** and **M3**: 1 μM; concentration of BSA: 1 μM.

implies that the structure of BSA may have not completely transformed to its original conformation but a conformation that is different from the native one, which has a low binding capacity for **M2** molecules. In the cooling process, the fluorescence of the BSA + **M3** system enhanced steeply and monotonously, and the intensity was evidently higher than the original state (Fig. 5B, blue squares). These spectral changes indicate that the BSA refolding process in the cooling run does not backtrack the unfolding process by heating. The refolded BSA has a new intermediate conformation that has a special domain(s) to accommodate more **M3** molecules or has a stronger ability to restrict the intramolecular rotations or vibrations of **M3** when the temperature went down from 70 °C to 25 °C.

The "abnormal" fluorescent responses of the BSA + **M3** system in the cooling process may be caused by a certain possible damage to BSA at 70 °C.[26] In order to eliminate this possibility, we repeated the heating–cooling cycles by a procedure of heating the systems to 50 °C and subsequently cooling the system to room temperature. The emission behavior of BSA + **M2** was quite similar to that shown in Fig. 6A and S7.† The FL intensity of **M2** underwent a diminution in the heating process and largely recovered to its inception in the cooling process. In the heating process, the emission intensity of **M3** exhibited a monotonous decrease before 42 °C, but an evident emission enhancement was recorded as the temperature reached to about 45 °C and higher. In the cooling process, a distinct and durative enhancement of emission was observed (Fig. 6B and S8†). Based on these data, it is reckoned that there exists a domain in the intermediate state (around 45 °C) that is able to effectively bind with **M3**. This domain may be buried in the native state of BSA, and thus it is inaccessible to be bound by **M3**. When BSA is converted to the intermediate state with rising temperature, the domain is exposed to the outside and becomes accessible.

The reversible and irreversible structural alterations of BSA were previously described on the basis of a two-step model.[27] It was reported that increasing the

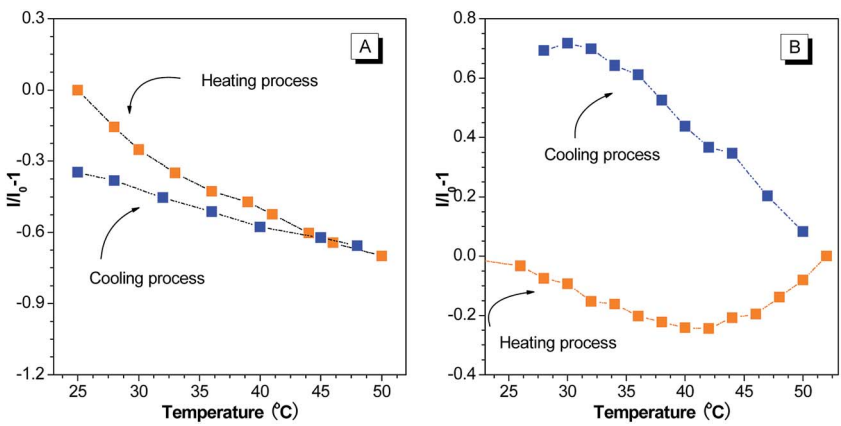

Fig. 6 Plots of the relative fluorescent intensities (I/I_0) of the (A) BSA + **M2** and (B) BSA + **M3** systems in PBS buffer (pH = 7.4) as a function of temperature in the heating (from 25 °C to 52 °C, orange) and subsequent cooling processes (from 52 °C to 25 °C, blue). I_0 and I: the peak FL intensity of the system at 25 °C and at a different temperature. λ_{ex}: 330 nm for **M2** and 395 nm for **M3**; concentration of **M2** and **M3**: 1 μM; concentration of BSA: 1 μM.

temperature to around 50 °C led to a reversible separation of domains I and II, and heating to a higher temperature of 70 °C led to the irreversible unfolding (denaturation) of domains I and II.[27] At room temperature, both **M2** and **M3** bind to the same subdomain IIA of BSA in the native state, though they bear ion groups with opposite charges. Subdomain IIA will go through irreversible damage when the temperature exceeds 70 °C. When the conformation of the albumin reversibly adjusts to an intermediate state through changing the temperature to 50 °C, the already existing binding site, which selectively interacts with **M3** containing a cationic group, starts to function and combine with **M3**. It is inferred that the positively charged **M3** binds to domain I of BSA in the intermediate state since domain I, which has a strong negative charge, can serve as a suitable binding site for cationic probes.[28]

Unfolding induced by guanidine hydrochloride and urea

The different responses of **M2** and **M3** to the temperature-induced unfolding and refolding processes of BSA suggest that the ligand binding behaviours of BSA actually have something to do with electrostatic interaction between the host and guest. In order to obtain further understanding of these processes, a study of the chemical denaturation of BSA induced by guanidine hydrochloride (GndHCl) was carried out by monitoring variations in the fluorescent spectral features of **M2** and **M3** in the presence of BSA, since it has been shown that some chemicals including GndHCl can cause BSA unfolding.[29] Fig. 7, S9 and S10† display the plots of the emission maxima of **M2** and **M3** in BSA buffer solution together with GndHCl in different concentrations. As a whole, the emission intensity becomes weaker and weaker with a gradual increase in the amount of denaturant. This trend suggests that the probe molecules are released from the hydrophobic

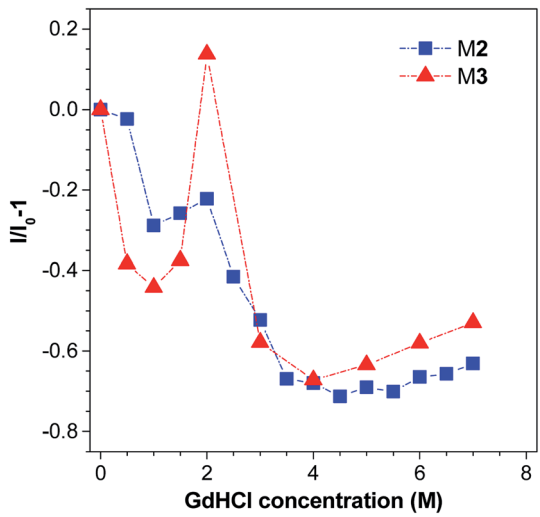

Fig. 7 Effect of GndHCl on the relative FL intensity (I/I_0) of **M2** and **M3** in the presence of BSA in PBS buffer (pH = 7.4). I_0 and I: the peak FL intensity of the sample without GndHCl and with different concentrations of GndHCl. λ_{ex}: 330 nm for **M2** and 395 nm for **M3**. Concentration of **M2** and **M3**: 1 μM; concentration of BSA: 1 μM.

pockets of BSA due to the denaturation induced by GndHCl, which can be mainly ascribed to the structural loss of subdomain IIA.

In detail, several turning points have been revealed in the plots. As shown in Fig. 6, the peak fluorescence intensity displays a transition step at a GndHCl concentration of 1.0 M for both **M2** and **M3**. Before this GndHCl concentration, the peak fluorescence intensity drops monotonously. Afterwards, the fluorescence intensity begins to increase and reaches its crest at around a GndHCl concentration of 2.0 M, which is followed by a secondary intensity decrease. When the GndHCl concentration increases to about 4.0 M, the fluorescence of the system demonstrates a small enhancement. The significant fluorescence enhancement at a GndHCl concentration of 2.0 M can be associated with the formation of a favorable rearrangement of subdomain IIA or a wider domain involving domains I and II. Such intermediates increase the binding of the probe molecules to the transformed BSA. A similar transition behavior was observed for the HSA + **M2** system and it was explained by the formation of a molten-globule intermediate,[17] which can provide larger or more hydrophobic regions to bind the probe molecules and thereby induce stronger emission.

To further validate the mutual existence of hydrophobic and electrostatic interactions in the target binding events occurring with BSA in different states, we examined the fluorescent responses of the BSA + **M2** and BSA + **M3** systems in the presence of urea. As shown in Fig. 8, for the BSA + **M2** system, the FL intensity goes down monotonously with the increase in urea concentration and levels off when the urea concentration reaches and exceeds 6 M (see also Fig. S11 and S12†). However, for the BSA + **M3** system, the FL intensity decreases in the urea concentration range of 1.0–3.0 M, and a sharp emission enhancement can be observed in the urea concentration range of 4.0–5.0 M. Finally, the emission intensity declines when the urea concentration is higher than 6.0 M.

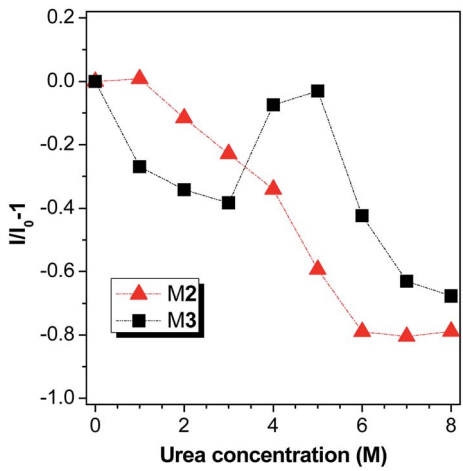

Fig. 8 Effect of urea concentration on the FL intensities (I/I_0) of **M2** or **M3** with BSA in PBS buffer (pH = 7.4). I_0 and I: the peak FL intensity of the sample without urea and with different concentrations of urea. λ_{ex}: 330 nm for **M2** and 395 nm for **M3**. Concentration of **M2** or **M3**: 1 μM; concentration of BSA: 1 μM.

Obviously, these data demonstrate the different responses of the BSA + **M2** and BSA + **M3** systems to GndHCl and urea. We tentatively associate the differences with the distinct denaturation effects on proteins between urea and GndHCl. Generally, GndHCl and urea have structural similarities, and both of them can denature or unfold proteins through hydrogen-bonding interaction between the N–H moiety of the urea and the carbonyl oxygen part of the protein backbone. As a charged denaturant, besides the hydrogen bonding effect, GndHCl would interact with the oppositely charged residues in the protein through electrostatic forces, which helps the protein unfolding process.[30] According to the literature, the intermediates with urea and GndHCl are similar to each other with a denatured domain III and the rearrangement of domains I and II. In the presence of around 1.0 M GndHCl, BSA attains a state with rearrangement and separation of domains I and II.[31] These conformational changes may lead to the release of partially encapsulated probe molecules into the buffer solution and the reduction of FL intensity. At around 1.5–2.0 M GndHCl, the deprivation of water molecules from the BSA surface results in the exposure of the hydrophobic residual sequences to the environment, thereby the probe molecules of **M2** and **M3** find cavities to bind on partially denatured BSA, which may possess a molten-globe state. Consequently, an increment of FL intensity has been observed in Fig. 7A and B at this GndHCl concentration range. The rearrangement of domain IA uncovers negatively charged residues like Asp, which helps the binding of positively charged **M3** to the hydrophobic molten-globe intermediate, thus the BSA + **M3** system shows higher FL intensity than the BSA + **M2** system. Further addition of GndHCl into the two systems causes a sharp decrease in FL intensity. At higher GndHCl concentrations (*e.g.* > 2 M), BSA is largely denatured and loses its native structure, becoming a random coil, thus forfeiting the original ability to bind **M2** and **M3**.

Without a net charge, urea shows a weaker denaturation ability than GndHCl. A higher concentration of urea is required to unfold BSA. As reported in the literature, the state in the presence of ~4.5 M urea has a partial loss of the native form of domain I along with the unfolding of domain II.[32] In this stage, the original pocket is totally deformed and the bonded **M2** or **M3** molecules are set free into the buffer solution. As a result, the FL intensity evidently declines (Fig. 8). At the same time, the deformation of domain I liberates Asp residues, and this form exhibits a strong affinity to positively charged **M3** probes, which induces the enhancement of FL intensity of **M3** in the presence of over 4.5 M urea. This behavior has not been observed in the case of GndHCl, because GndHCl is a denaturant with a positive charge, which effectively shields the electrostatic interaction between cationic **M3** and the negatively charged net of the deformed domain I.

The above results and discussion indicate that electrostatic interaction between the probe and deformed BSA plays a crucial role in the denaturing process. To offer further proof, we then examined the effect of pH, especially under acidic conditions, on the structural changes of BSA by monitoring the fluorescent features of the two probes. The pH values of the two systems have been altered from 7.4 to 2.0, and the variation of the FL intensity recorded at the peak emission wavelength with pH are summarized in Fig. 9 (see also Fig. S13 and S14†). Both **M2** and **M3** show negligible FL intensity change in the pH range examined in the absence of BSA. For the BSA + **M2** system, in the

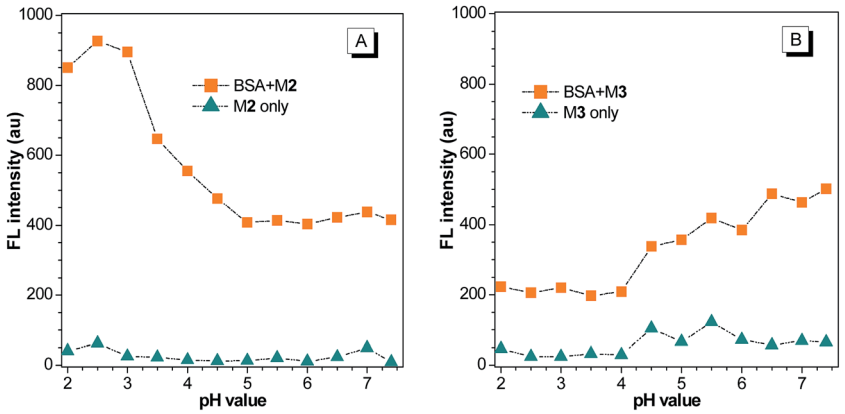

Fig. 9 Variation of FL intensity of (A) **M2** and (B) **M3** in the presence or absence of BSA in PBS buffer with different pH values (2.0–7.4). λ_{ex}: 330 nm for **M2** and 395 nm for **M3**. Concentration of **M2** and **M3**: 1 μM; concentration of BSA: 1 μM.

range of pH from 7.4 to 4.5, the FL intensity shows little change. When the pH is reduced further to below 4.5, a gradual emission enhancement occurs and the intensity has been finally doubled at pH 2.0. When it comes to the system of BSA + **M3**, along with the pH being altered from 7.4 to 2.0, the FL intensity undergoes a decrease until the pH drops to about 4.5 and then it levels off. The fluorescent behaviors of the two systems can be divided into two pH-relevant regions, and the breakpoint localizes at around the isoelectric point of BSA, which is approximately at 4.9.[33] When the pH is lower than this point, the native BSA begins to isomerize to a partially-extended 'molten globule' state, which is predominantly populated at pH 3,[34] and the basic residues such as Arg and Lys are positively charged and repel the binding of positively charged **M3** but attract negatively charged **M2**. Consequently, below the breakpoint, the BSA + **M2** (Fig. 9A) and BSA + **M3** (Fig. 9B) systems display enhanced and weakened FL emission respectively.

Conclusions

In summary, the binding behaviours of BSA towards external species in its native, intermediate and unfolded states have been investigated by using two AIE-active fluorescent probes, **M2** and **M3**, which are intentionally designed to bear negative and positive charges, respectively. On account of their aggregation-induced emission properties, **M2** and **M3** show remarkably enhanced emission as they bind to BSA. According to the Stern–Volmer equation and FRET principle, it was estimated that BSA could bind to one **M2** or one **M3** probe, and the binding constants of **M2** and **M3** to native BSA were measured to be 5.50×10^7 and 1.38×10^6 L mol^{-1}, respectively. The displacement effects of site-specific binding ligands (myristic acid and warfarin) on the probes indicated that both **M2** and **M3** selectively bound to the subdomain IIA of BSA. Hydrophobic interaction was the driving force of the binding process, regardless of the negative and positive charges carried by the probes.

When **M2** and **M3** were used to probe the BSA unfolding process induced by thermal treatment and by the addition of denaturants urea or GndHCl, the differently charged probes showed drastically different fluorescent responses. As subdomain IIA rearranged and separated from the other domains, its affinity to **M2** and **M3** evidently attenuates, for the hydrophobic pocket holding the probes was destroyed. When BSA went through a partial unfolding process in response to external stimuli, the buried pockets or cavities (domain I) in BSA become a favourable site for the specific binding of cationic **M3**, because the negatively charged residues were exposed to the surroundings at this stage. In the cooling-induced refolding process, the formation of the hydrophobic pocket at subdomain IIA accommodated both **M2** and **M3**, thus lighting up the emission from the probes. Meanwhile, the electrostatic interaction between cationic **M3** and the anionic residue in the unfolded domain I allowed the excessive encapsulation of **M3** into the pocket of domain I in the cooling run. Therefore, marked enhancement emission from **M3** was recorded.

The experimental results reported herein are quite distinct from the data previously reported for fluorescent probes. In addition to hydrophobic interactions, by which BSA and other albumins to play their primary transport role, electrostatic interactions also play a crucial role in their response towards charged species. The fluorescent behaviours of BSA towards the two ionic probes indicate that **M2** and **M3** are efficient reporters of the folding, unfolding and refolding of BSA. Their emission changes disclose useful information about the loading and release of charged species, which will be instructive to studies on pharmaceutics or drug pharmacokinetics.

Acknowledgements

This work was financially supported by the key project of the Ministry of Science and Technology of China (2013CB834704), the National Science Foundation of China (51573158), and the Research Grants Council of Hong Kong (16301614, N_HKUST604/14 and N_HKUST620/11). J. Z. Sun thanks the financial support from Zhejiang Innovative Research Team Program (2013TD02). A. Qin and B. Z. Tang thank the support from Guangdong Innovative Research Team Program (201101C0105067115).

Notes and references

1 G. Fanali, A. di Masi, V. Trezza, M. Marino, M. Fasano and P. Ascenzi, *Mol. Aspects Med.*, 2012, **33**, 209.

2 (*a*) F. Yang, Y. Zhang and H. Liang, *Int. J. Mol. Sci.*, 2014, **15**, 3580; (*b*) A. Varshney, P. Sen, E. Ahmad, M. Rehan, N. Subbarao and R. H. Khan, *Chirality*, 2010, **22**, 77; (*c*) U. Kragh-Hansen, *Biochim. Biophys. Acta*, 2013, **1830**, 5535.

3 (*a*) A. A. Bhattacharya, T. Grüne and S. Curry, *J. Mol. Biol.*, 2000, **303**, 721; (*b*) I. Petitpas, T. Grüne, A. A. Bhattacharya and S. Curry, *J. Mol. Biol.*, 2001, **314**, 955; (*c*) S. Curry, H. Mandelkow, P. Brick and N. Franks, *Nat. Struct. Biol.*, 1998, **5**, 827.

4 (*a*) A. Ahmed-Ouameur, S. Diamantoglou, M. R. Sedaghat-Herati, S. Nafisi, R. Carpentier and H. A. Tajmir-Riahi, *Cell Biochem. Biophys.*, 2006, **45**, 203; (*b*) S. Naveenraj and S. Anandan, *J. Photochem. Photobiol., C*, 2013, **14**, 53.

5 (*a*) F. A. de Wolf and G. M. Brett, *Pharmacol. Rev.*, 2000, **52**, 207; (*b*) F. Yang, C. Bian, L. Zhu, G. Zhao, Z. Huang and M. Huang, *J. Struct. Biol.*, 2007, **157**, 348.

6 (*a*) A. Bujacz, *Acta Crystallogr., Sect. D: Biol. Crystallogr.*, 2012, **68**, 1278; (*b*) K. A. Majorek, P. J. Porebski, A. Dayal, M. D. Zimmerman, K. Jablonska, A. J. Stewart, M. Chruszcz and W. Minor, *Mol. Immunol.*, 2012, **52**, 174.

7 (*a*) Y.-J. Hu, Y. Liu, L.-X. Zhang, R.-M. Zhao and S.-S. Qu, *J. Mol. Struct.*, 2005, **750**, 174; (*b*) S. Shah, A. Sharma and M. N. Gupta, *Anal. Biochem.*, 2006, **351**, 207; (*c*) L. Hu, S. Han, S. Parveen, Y. Yuan, L. Zhang and G. Xu, *Biosens. Bioelectron.*, 2012, **32**, 297; (*d*) A. B. Kayitmazer, S. P. Strand, C. Tribet, W. Jaeger and P. L. Dubin, *Biomacromolecules*, 2007, **8**, 3568; (*e*) C. M. Valmikinathan, S. Defroda and X. Yu, *Biomacromolecules*, 2009, **10**, 1084.

8 U. Anand and S. Mukherjee, *Biochim. Biophys. Acta*, 2013, **1830**, 5394.

9 (*a*) L. A. MacManus-Spencer, M. L. Tse, P. C. Hebert, H. N. Bischel and R. G. Luthy, *Anal. Chem.*, 2010, **82**, 974; (*b*) C. Li and G. J. Pielak, *J. Am. Chem. Soc.*, 2009, **131**, 1368; (*c*) T. Wu, Q. Wu, S. Guan, H. Su and Z. Cai, *Biomacromolecules*, 2007, **8**, 1899; (*d*) Q. Yang, J. Liang and H. Han, *J. Phys. Chem. B*, 2009, **113**, 10454; (*e*) A. Valstar, M. Almgren and W. Brown, *Langmuir*, 2000, **16**, 922.

10 (*a*) C. A. Royer, *Chem. Rev.*, 2006, **106**, 1769; (*b*) F.-L. Cui, J.-L. Wang, Y.-R. Cui and J.-P. Li, *Anal. Chim. Acta*, 2006, **571**, 175; (*c*) V. S. Jisha, K. T. Arun, M. Hariharan and D. Ramaiah, *J. Am. Chem. Soc.*, 2006, **128**, 6024; (*d*) J. Jayabharathi, V. Thanikachalam, K. Saravanan and M. V. Perumal, *Spectrochim. Acta, Part A*, 2011, **79**, 1240.

11 (*a*) J. R. Lakowicz, J. Malicka, S. D'Auria and I. Gryczynski, *Anal. Biochem.*, 2003, **320**, 13; (*b*) Y. Suzuki and K. Yokoyama, *J. Am. Chem. Soc.*, 2005, **127**, 17799; (*c*) D. Ding, K. Li, B. Liu and B. Z. Tang, *Acc. Chem. Res.*, 2013, **46**, 2441.

12 H. Tong, Y. Hong, Y. Dong, M. Häußler, J. W. Y. Lam, Z. Li, Z. Guo and B. Z. Tang, *Chem. Commun.*, 2006, 3705.

13 J. Mei, Y. Hong, J. W. Y. Lam, A. Qin, Y. Tang and B. Z. Tang, *Adv. Mater.*, 2014, **26**, 5429.

14 H. Tong, Y. Hong, Y. Dong, M. Häußler, Z. Li, J. W. Y. Lam, Y. Dong, H. H.-Y. Sung, I. D. Williams and B. Z. Tang, *J. Phys. Chem. B*, 2007, **111**, 11817.

15 W. Z. Yuan, H. Zhao, X. Y. Shen, F. Mahtab, J. W. Y. Lam, J. Z. Sun and B. Z. Tang, *Macromolecules*, 2009, **42**, 9400.

16 (*a*) X. Wang, J. Hu, G. Zhang and S. Liu, *J. Am. Chem. Soc.*, 2014, **136**, 9890; (*b*) G. N. Zhao, B. Tang, Y. Q. Dong, W. H. Xie and B. Z. Tang, *J. Mater. Chem. B*, 2014, **2**, 5093; (*c*) H. Shi, J. Liu, J. Geng, B. Z. Tang and B. Liu, *J. Am. Chem. Soc.*, 2012, **134**, 9569; (*d*) Y. Hong, L. Meng, S. Chen, C. W. Tung, L.-T. Da, M. Faisal, D.-A. Silva, J. Liu, J. W. Y. Lam, X. Huang and B. Z. Tang, *J. Am. Chem. Soc.*, 2012, **134**, 1680.

17 Y. Hong, C. Feng, Y. Yu, J. Liu, J. W. Y. Lam, K. Q. Luo and B. Z. Tang, *Anal. Chem.*, 2010, **82**, 7035.

18 (*a*) J. K. Jin, X. J. Chen, Y. Liu, A. Qin, J. Z. Sun and B. Z. Tang, *Acta Polym. Sin.*, 2011, **9**, 1079; (*b*) T. Hu, X. J. Chen, B. C. Yao, A. Qin, J. Z. Sun and B. Z. Tang, *Chem. Commun.*, 2015, **51**, 8849.

19 R. F. Chen, *J. Biol. Chem.*, 1967, **242**, 173.

20 (*a*) A. Sulkowska, *J. Mol. Struct.*, 2002, **614**, 227; (*b*) Y.-Q. Wang, H.-M. Zhang, G.-C. Zhang, W.-H. Tao and S.-H. Tang, *J. Lumin.*, 2007, **126**, 211.
21 (*a*) B. K. Paul, A. Samanta and N. Guchhait, *J. Phys. Chem. B*, 2010, **114**, 6183; (*b*) N. Chadborn, J. Bryant, A. J. Bain and P. O'Shea, *Biophys. J.*, 1999, **76**, 2198.
22 O. K. Abou-Zied and O. I. K. Al-Shihi, *J. Am. Chem. Soc.*, 2008, **130**, 10793.
23 (*a*) S. Curry, P. Brick and N. P. Franks, *Biochim. Biophys. Acta*, 1999, **1441**, 131; (*b*) D. P. Cistola, D. M. Small and J. A. Hamilton, *J. Biol. Chem.*, 1987, **262**, 10980; (*c*) J. A. Hamilton, S. Era, S. P. Bhamidipati and R. G. Reed, *Proc. Natl. Acad. Sci. U. S. A.*, 1991, **88**, 2051.
24 (*a*) G. Sudlow, D. J. Birkett and D. N. Wade, *Mol. Pharmacol.*, 1975, **11**, 824; (*b*) G. Sudlow, D. J. Birkett and D. N. Wade, *Mol. Pharmacol.*, 1976, **12**, 1052.
25 (*a*) L. Fu, S. Villette, S. Petoud, F. Fernandez-Alonso and M. Saboungi, *J. Phys. Chem. B*, 2011, **115**, 1881; (*b*) G. Graziano, *Phys. Chem. Chem. Phys.*, 2010, **12**, 14245.
26 Y. Moriyama, E. Watanabe, K. Kobayashi, H. Harano, E. Inui and K. Takeda, *J. Phys. Chem. B*, 2008, **112**, 16585.
27 (*a*) D. Banerjee and S. K. Pal, *Photochem. Photobiol.*, 2008, **84**, 750; (*b*) Y. Moriyama, Y. Kawasaka and K. Takeda, *J. Colloid Interface Sci.*, 2003, **257**, 41; (*c*) C. Honda, H. Kamizono, T. Samejima and K. Endo, *Chem. Pharm. Bull.*, 2000, **48**, 464.
28 (*a*) A. Chakrabarty, A. Mallick, B. Haldar, P. Das and N. Chattopadhyay, *Biomacromolecules*, 2007, **8**, 920; (*b*) U. Kragh-Hansen, *Pharmacol. Rev.*, 1981, **33**, 17.
29 (*a*) A. Chowdhury, V. Banerjee, R. Banerjee and K. P. Das, *Biopolymers*, 2014, **101**, 549; (*b*) A. A. A. Halim, H. A. Kadir and S. Tayyab, *J. Biochem.*, 2008, **144**, 33; (*c*) O. D. Monera, C. M. Kay and O. S. Hodges, *Protein Sci.*, 1994, **3**, 1984.
30 (*a*) W. K. Lim, J. Rösgen and S. W. Englandera, *Proc. Natl. Acad. Sci. U. S. A.*, 2009, **106**, 2595; (*b*) R. Kumaran and P. Ramamurthy, *J. Fluoresc.*, 2011, **21**, 1499.
31 (*a*) U. Anand, C. Jash and S. Mukherjee, *Phys. Chem. Chem. Phys.*, 2011, **13**, 20418; (*b*) B. Ahmad, M. Z. Ahmed, S. K. Haq and R. H. Khan, *Biochim. Biophys. Acta*, 2005, **1750**, 93.
32 (*a*) S. Tayyab, N. Sharma and M. M. Khan, *Biochem. Biophys. Res. Commun.*, 2000, **277**, 83; (*b*) M. Y. Khan, S. K. Agarwal and S. Hangloo, *J. Biochem.*, 1987, **102**, 313; (*c*) N. Ahmad and M. A. Qasim, *Eur. J. Biochem.*, 1995, **227**, 563.
33 Y. Li, J. Lee, J. Lai, L. An and Q. Huang, *J. Phys. Chem. B*, 2008, **112**, 3797.
34 M. Bhattacharya, N. Jain, K. Bhasne, V. Kumari and S. Mukhopadhyay, *J. Fluoresc.*, 2011, **21**, 1083.